DOI:10.24850/j-tyca-2018-05-01
Articles

Temporal evolution of hydrological drought in Argentina and its relationship with macroclimatic indicators
Evolución temporal de las sequías hidrológicas en Argentina y su relación con indicadores macroclimáticos

Erica Díaz[1]
Marcelo García[2]
Andrés Rodríguez[3]
Oscar Dölling[4]
Santiago Ochoa[5]
Juan Bertoni[6]

[1]Universidad Nacional de Córdoba, Córdoba, Argentina, erica.betiana.diaz@unc.edu.ar
[2]Universidad Nacional de Córdoba, Córdoba, Argentina, carlos.marcelo.garcia@unc.edu.ar
[3]Universidad Nacional de Córdoba, Córdoba, Argentina, andres.rodriguez@unc.edu.ar
[4]Universidad Nacional de San Juan, San Juan, Argentina, odolling@unsj.edu.ar
[5]Universidad Nacional de Córdoba, Córdoba, Argentina, santiago.ochoa@unc.edu.ar
[6]Universidad Nacional de Córdoba, Córdoba, Argentina, jcbertoni@unc.edu.ar

Correspondence author: Erica Díaz, erica.betiana.diaz@unc.edu.ar

Abstract

This paper identifies multiannual periodicities of historical mean annual flow series of 14 rivers in Argentina and 10 macro-climatic indices using spectral analysis. The estimation of dominant frequencies in the analyzed time series allows understanding the time

scale of the processes involved in the hydrological cycles. Through spectral analysis, it was found that high, low and medium frequency fluctuations contribute, in different percentages, to the flow variability. Then, these results were compared to results of similar analyses performed on time series of macro-climatic indices to calculate the relation of the evolution of these indices with flow discharge series. These results constitute an important step toward implementing conceptual and forecasting models of deficit and excess of surface water in fluvial systems for planning and management of water resources.

Keywords: Hydrological drought, macro-climatic indices.

Resumen

En este trabajo se identifican, a través de un análisis espectral, las periodicidades plurianuales en las series históricas de caudales medios anuales escurridos en 14 sistemas fluviales de la República Argentina y en 10 indicadores macroclimáticos. La identificación de las frecuencias de tiempo dominantes en las series de caudales escurridos permite comprender la escala temporal de evolución de los procesos físicos que intervienen en los ciclos hidrológicos. En el análisis realizado se encontró que existe en todas las series históricas de caudales medios anuales escurridos fluctuaciones de alta, baja y media frecuencia, que aportan, con distinta significancia, a la variabilidad temporal de los caudales escurridos. Los resultados se contrastaron con los obtenidos en el análisis de series de indicadores macroclimáticos, para saber si existía relación de la evolución de tales indicadores con las series de caudales. Los resultados alcanzados permiten avanzar en la generación de modelos conceptuales y de pronósticos implementados para prever los años de déficit y excesos hídricos en los sistemas fluviales, lo que constituye una herramienta importante para la planificación y gestión de los recursos hídricos.

Palabras clave: sequías hidrológicas, indicadores macroclimáticos.

Received: 04/11/2016
Accepted: 03/04/2018

Introduction

For adequate management of water resources, proper planning and management of water resources requires knowledge about the variability of supply and demand of resources in a region. Knowledge of the temporal and spatial evolution of available water resources is important for decision making.

The situations of extreme hydrological periods of excess water and water scarcity represent threats to society. In particular, droughts are a complex phenomenon that affects the development and use of water resources in a region (Fernández, 1997). The knowledge of drought characteristics (frequency of occurrence, duration, spatial extension, intensity and magnitude) and their relation with the macro-climatic phenomena helps the generation of prediction models in the medium- and long-term. These would help the efficient management of water resources during periods of scarcity.

Previous work carried out by the authors identified and characterized hydrological droughts in Argentina (Díaz, Rodríguez, Dölling, Bertoni, & Smrekar, 2016). This work identifies multiannual periodicities of flows series for fluvial systems in Argentina, as well macro-climatic indices, using spectral analysis. The dominant frequencies (characterizing the multiannual periodicities) in the flow series contributes to understanding the temporal evolution of the processes involved in the hydrological cycles. Also, it helps to generate conceptual models that explain these processes and to develop forecast models at different scales to predict years with water deficits.

Study area

The study area includes 14 basins in the Central, North and Cuyo regions in Argentina. Table 1 and Figure 1 describe its main characteristics.

Table 1. Summary of hydrological and geographical characteristics of the basins analysed.

Identifier	Basin	Gauging station		Contribution area to the station	Module [m³/s]	Data Period
		Denomination	Location			

			South Latitude	West Longitude	Altitude [masl]	[Km²]		
1	San Juan	San Juan - Km 47,3	31°30'59"	68°56'25"	934	25660	65	1909-2013
2	Mendoza	Guido	32°54'55"	69°14'16"	1408	8180	45,6	1956-2013
3	Atuel	La Angostura	35°05'57"	68° 52'26"	1302	3800	35.4	1905-2013
4	Colorado	Buta Ranquil	37°04'34"	69°44'48"	850	15300	148	1940-2013
5	Ctalamochita	Embalse	32°10'00"	64°23'00"	650	3300	27,1	1913-1984
6	Xanaes	Los Molinos	31°48'10"	64°30'59"	770	980	9,5	1936-2009
7	Anisacate	Santa Ana	31°40'00"	64°34'00"	900	465	4,83	1925-1980
8	Suquía	San Roque	31°22'00"	64°27'00"	650	1350	10	1926-2011
9	Dulce	La Escuela	27°30' 00"	64°51' 00"	265	19700	82,2	1925-2013
10	Juramento	Cabra Corral	25°16'19"	65°19'47"	945	32885	29,5	1934-2013
11	Bermejo	Pozo Sarmiento	23°13'00"	64°12'00"	296	25000	446	1952-2013
12	Pilcomayo	La Paz	22°22'41"	62°31'21"	230	96000	237	1941-2013
13	Paraná	Corrientes	27°28'30"	58°49'60"	52	1950000	17189	1906-2013
14	Salado	Ruta Provincial 70	31°29'28"	60°46'50"	17	29700	137	1954-2013

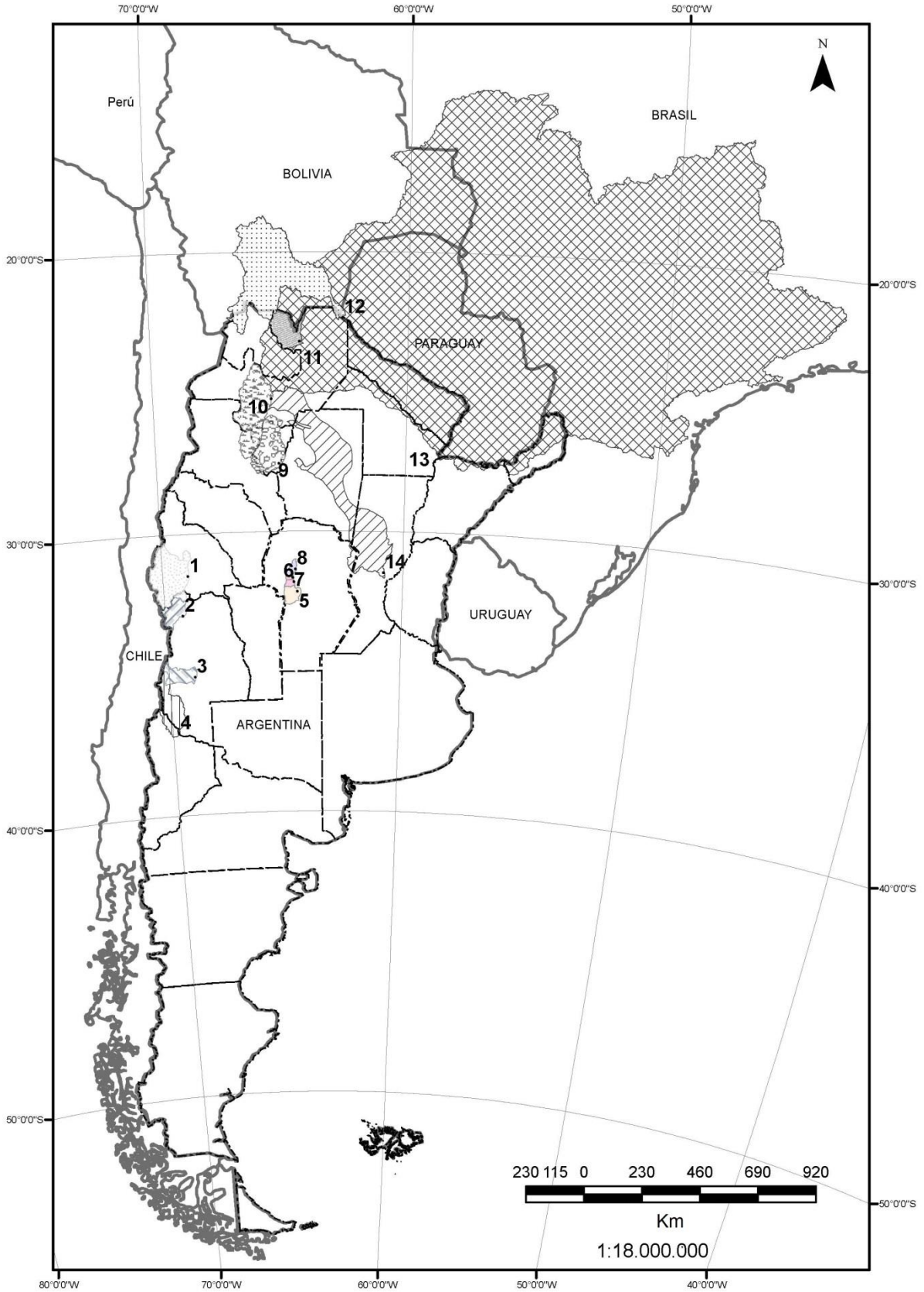
70°0'0"W
60°0'0"W
50°0'0"W
N
Perú
BRASIL
BOLIVIA
20°0'0"S
12
11
PARAGUAY
10
9
13
30°0'0"S
1
8
6
7
5
14
2
URUGUAY
CHILE
3
4
ARGENTINA
40°0'0"S
50°0'0"S
230 115 0 230 460 690 920
Km
1:18.000.000
80°0'0"W
70°0'0"W
60°0'0"W
50°0'0"W
40°0'0"W

Figure 1. Location of the basins analyzed. The numbers correspond to the identifier shown in Table 1.

The flow series analyzed correspond to basins located in Central, North, NOA and Cuyo regions in Argentina, shown in Figure 1. The rivers have different characteristics in terms of basin location, mean flow, area of contribution and annual volume of water contribution (see Table 1).

San Juan River basin covers a great percentage of the province of San Juan, and a small portion of northern Mendoza province. Surface runoff comes mainly from thaw of Andean glaciers, which is the main source of aquifer recharge.

Mendoza River basin is located in the northwest of the Mendoza province and part of the province of San Juan. This basin drains 90 km from the front of the Andes mountain range. The waters of this river come mostly from thaw.

Atuel River is the fifth tributary of Desaguadero River. It has a snowy regime, although it receives rainwater. It has an approximate length of 600 km. Its feeding basin is located at more than 3 000 meters above sea level in the Andes.

The Colorado River basin includes four eco-regions with very varied relief and a rainfall regime, with a mean annual rainfall from 100 mm to 600 mm (Subsecretaría de Recursos Hídricos, 2010). It is a snowy-rainy basin.

The Ctalamochita River basin belongs to Carcaraña River basin, ending in the Plata basin. It begins on the eastern slopes of Sierras Grandes (province of Cordoba). At present, the Ctalamochita River is regulated by a chain of artificial reservoirs.

The Xanaes River basin starts in the confluence of the Anisacate and Los Molinos rivers. The Anisacate River results from the union of La Suela and San José rivers. It crosses the Sierras Chicas Mountains in a narrow canyon, as a retrograde river.

The Suquía River basin is approximately 6 000 km^2, located near Mar Chiquita lagoon. In the study location, the area of the Suquía River basin is 1 350 km^2. These are typical mountain rivers, where streamflow variations respond directly to rainfall variations.

The Dulce River basin includes the provinces of Tucumán, Salta and Catamarca. It presents an average annual rainfall of 800 mm and it is considered to be a humid climate.

Pasaje-Juramento River basin begins in the snow peaks of Cachi and Acay mountains (4 895 meters above sea level). The upper and

middle basins are located in the province of Salta. The Juramento River is regulated by the General Belgrano Dam (Cabra Corral).

Bermejo River basin is part of the Del Plata hydrographic basin, and together with the Pilcomayo River, it is the main tributary of Paraguay River. The upper basin of Bermejo River is located in the northwest portion of Argentina and the south-southeast region of Bolivia. The main annual rainfall varies from 200mm in the west to 1 400 mm in the center of the basin.

Pilcomayo is a mountain river that has its upper basin in the Bolivian Andes at more than 5 000 meters above sea level, passing in a NW-SE direction through the Andes. Throughout geological times, the river has been depositing a large part of the sediments that it transports in the Chaqueña plains, thus building a large alluvial fan.

The portion of the Paraná River basin located in the study area (Corrientes station) has an area of 1 950 000 Km^2. This basin is part of the Plata basin, one of the largest in the world. There is a shortage of rain in winter (June-August) in most of the basin. And heavy rains occur in summer, which are less in the west and in the regions located north of the tropic of Capricorn to the Brazilian Planalto. Towards the south it is characterized by abundant rainfall. The mean annual rainfall is 1 200mm (1961-1990) (Paoli & Schreider, 2000). Salado River basin belongs to Del Plata basin. The upper basin of Salado River begins in the eastern foothills of the Andes, in the province of Salta. Its main source is in the Sierra de los Pasos Grandes Mountain, almost immediately south of Acay's snowy hill. It is a river with a rainy-snowy regime.

Methodology and results

Spectral Analysis for Main Annual Streamflow Series

The spectral analysis consists of calculating the energy spectrums of the historical annual mean flow series to identify the dominant frequencies. In the spectral analysis, the mean flow series in the frequency domain are analyzed using the Fast Fourier Transform.

Then, the energy spectrum of the fluctuation is calculated using the following equation:

$$\boldsymbol{E} = \frac{2\Delta t}{N}[\boldsymbol{X_m}]^2 \qquad (1)$$

Where:

Δt: Time step (in this work it is equal to 1 year)

N: Data numbers in the series

$[X_m]^2$: Magnitude of the Fourier Transform

The following figures ((Figure 2, Figure 3, Figure 4, Figure 5, Figure 6, Figure 7, Figure 8, Figure 9, Figure 10, Figure 11, Figure 12, Figure 13, Figure 15 y Figure 15) show the mean annual flow series with their respective dimensionless energy spectrum (using the maximum energy value to nondimensionalize), highlighting the three frequencies considered as dominant in each spectrum (Table 2).

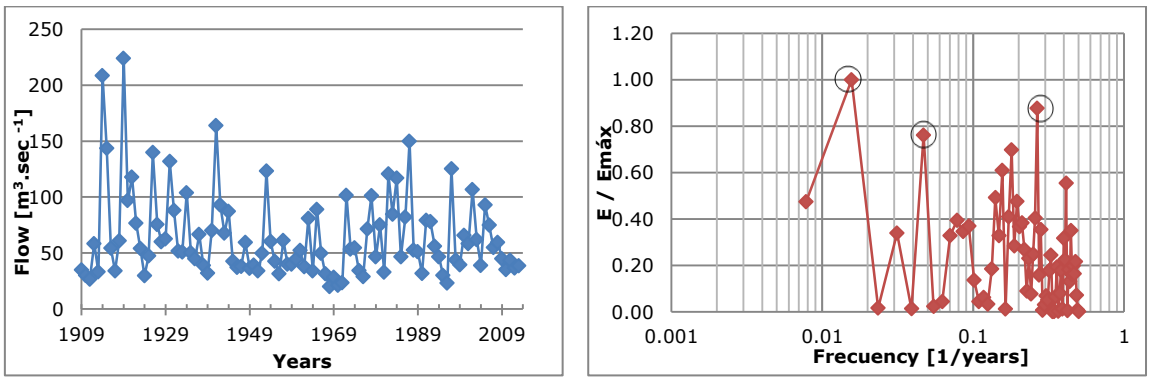

Figure 2. Time series and energy spectrum for mean annual flow of San Juan River.

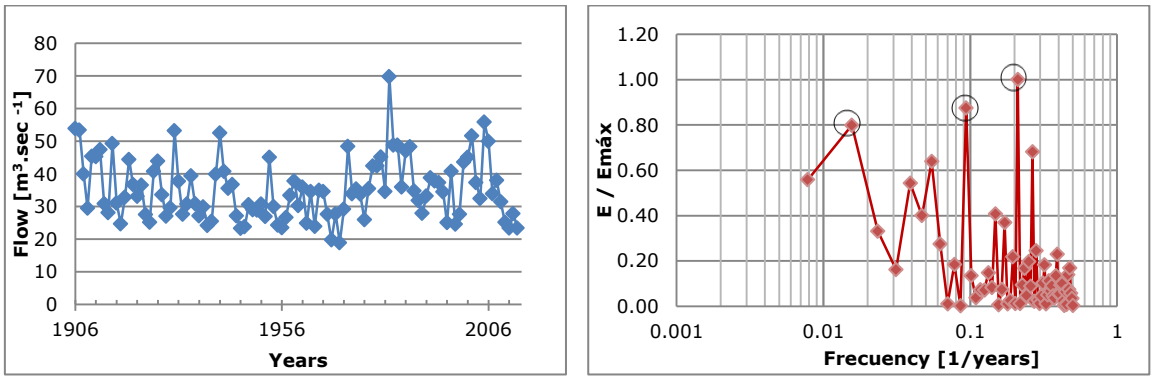

Figure 3. Time series and energy spectrum for mean annual flow of Atuel River.

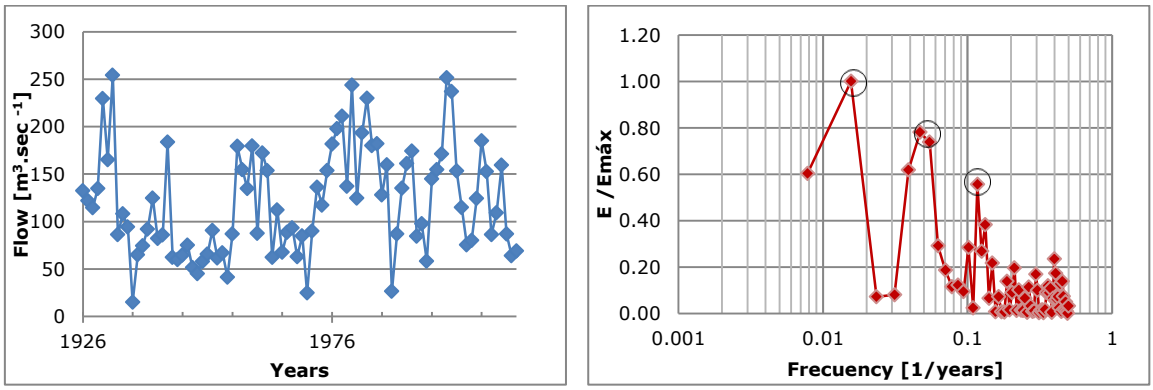

Figure 4. Time series and energy spectrum for mean annual flow of Dulce River.

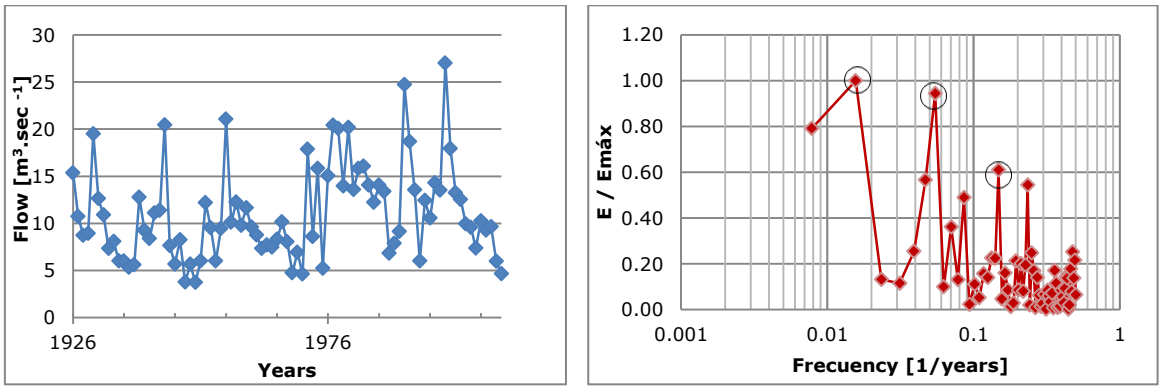

Figure 5. Time series and energy spectrum for mean annual flow of Suquia River.

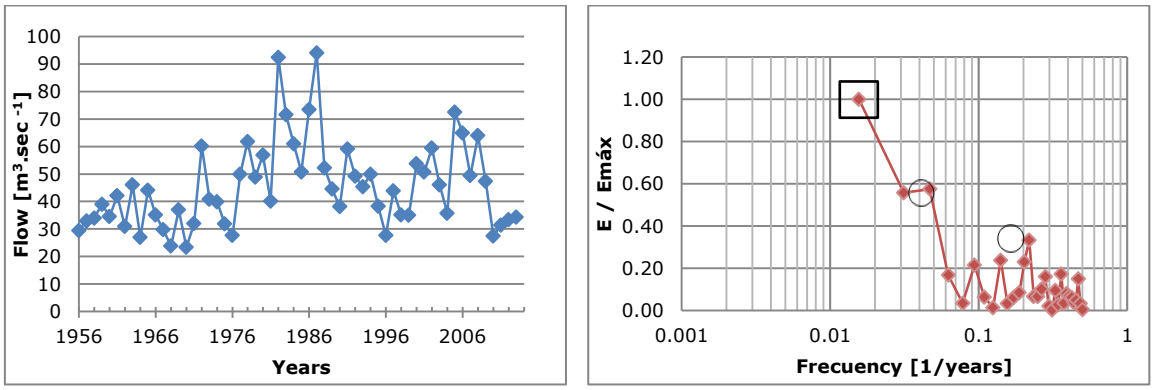

Figure 6. Time series and energy spectrum for mean annual flow of Mendoza River.

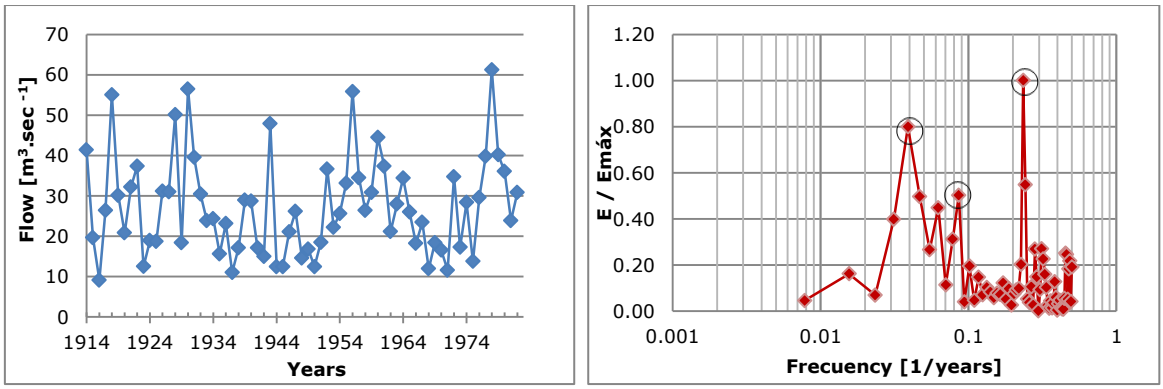

Figure 7. Time series and energy spectrum for mean annual flow of Catalamochita River.

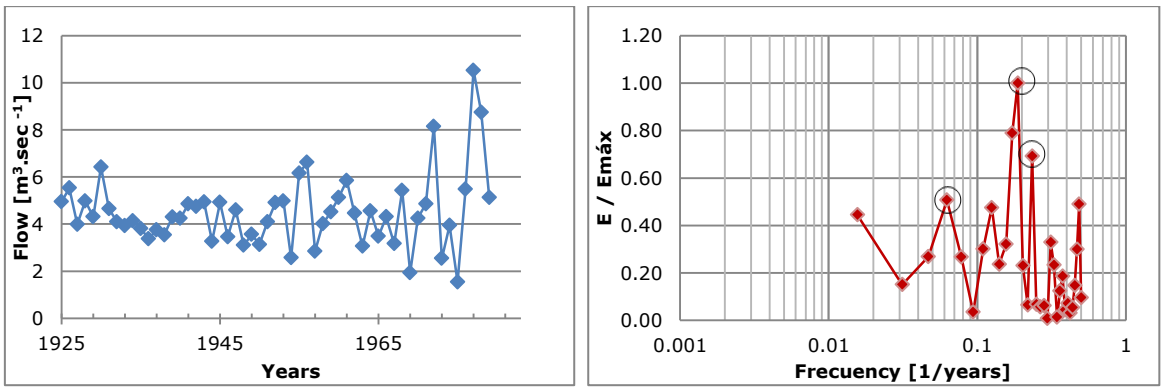

Figure 8. Time series and energy spectrum for mean annual flow of Anisacate River.

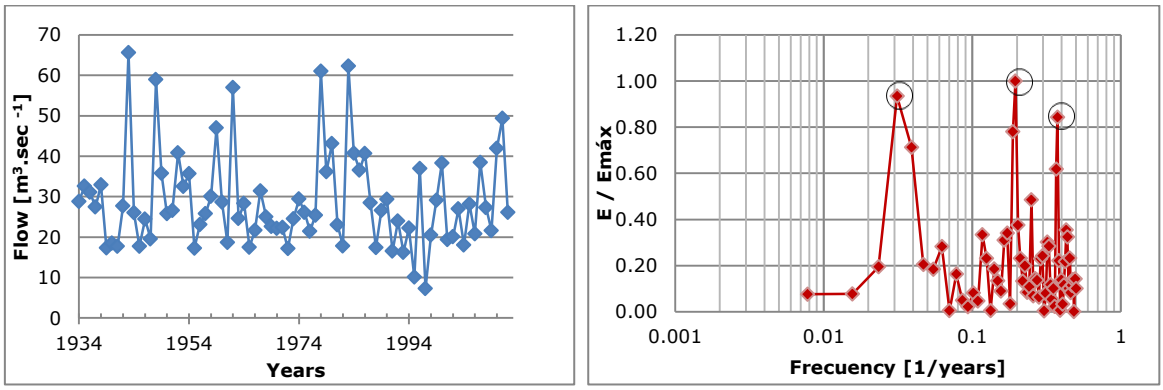

Figure 9. Time series and energy spectrum for mean annual flow of Juramento River.

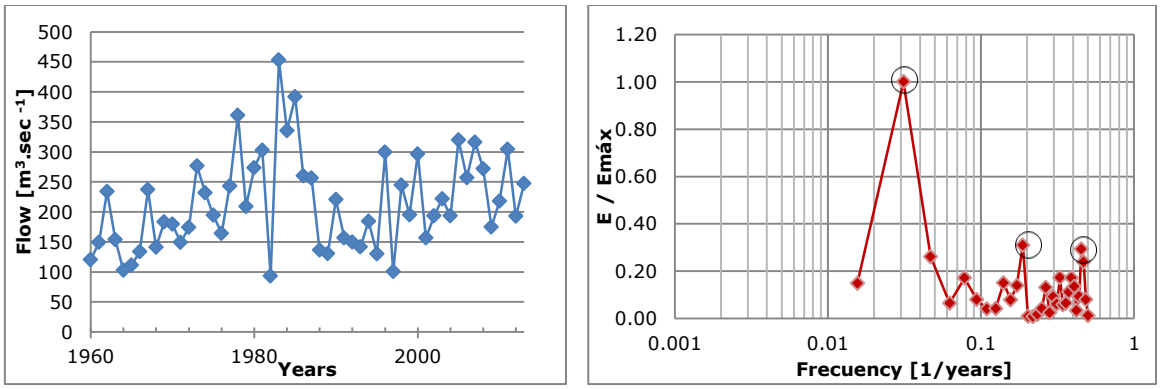

Figure 10. Time series and energy spectrum for mean annual flow of Pilcomayo River.

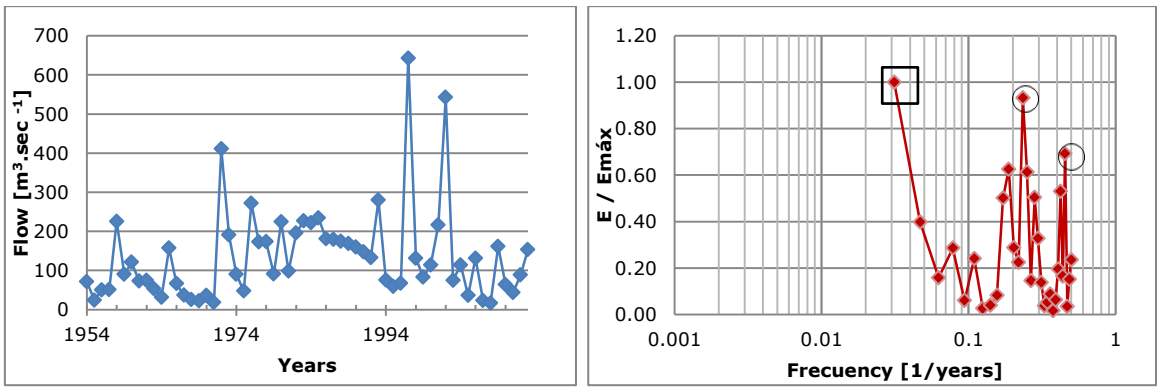

Figure 11. Time series and energy spectrum for mean annual flow of Salado River.

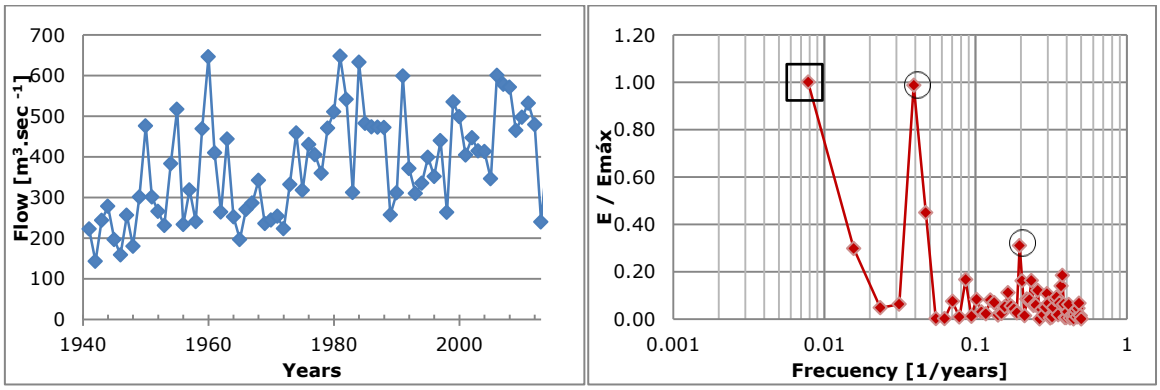

Figure 12. Time series and energy spectrum for mean annual flow of Bermejo River.

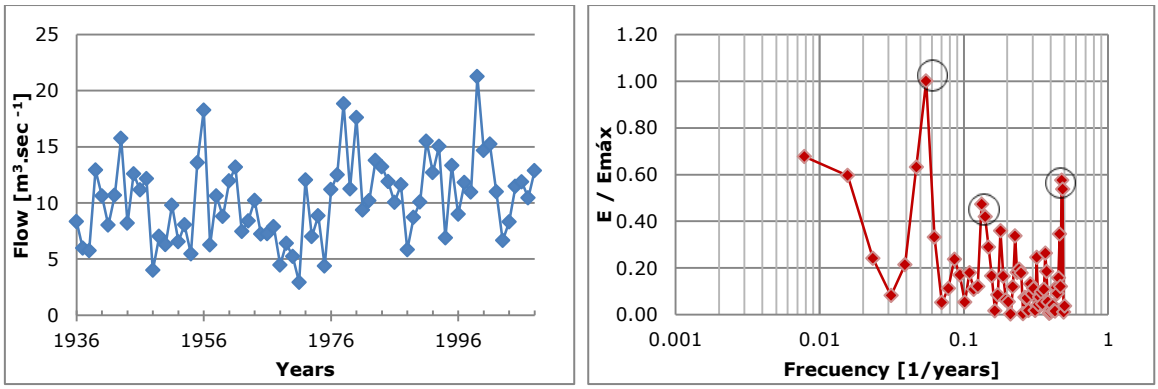

Figure 13. Time series and energy spectrum for mean annual flow of Xanaes River.

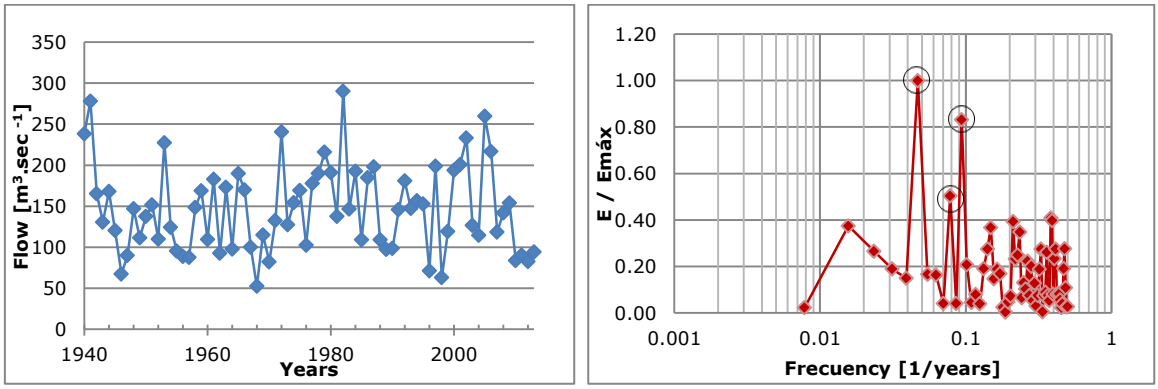

Figure 14. Time series and energy spectrum for mean annual flow of Colorado River.

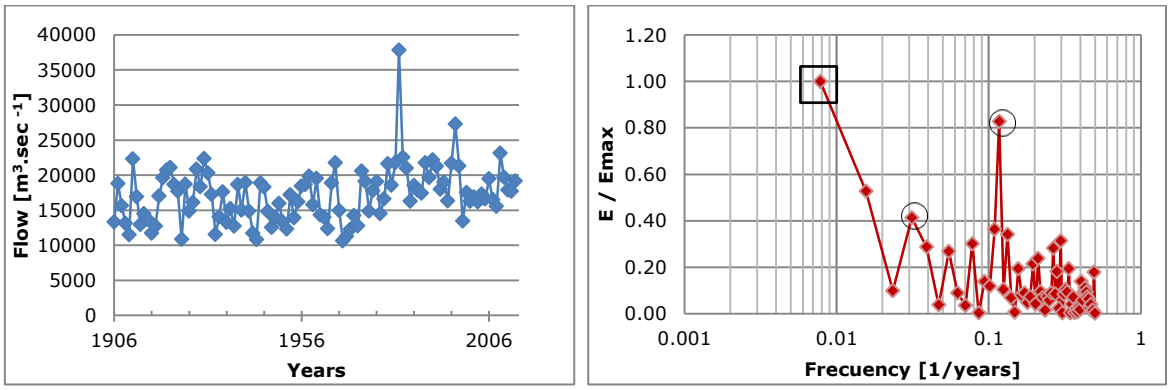

Figure 15. Time series and energy spectrum for mean annual flow of Parana River.

Table 2. Dominant frequencies and dimensionless energy spectrum (nondimensionalized with its maximum value) of each basin analyzed.

Basin	Maximum value selected			Second value selected		
	E / Emáx	Frecuency [1/year]	Period [Years]	E / Emáx	Frecuency [1/year]	Period [Year]
San Juan	0.88	0.27	3.8	0.76	0.05	21.3
Mendoza	0.33	0.22	21.3	0.23	0.20	4.6
Atuel	1.00	0.21	4.7	0.88	0.09	10.7
Colorado	1.00	0.05	21.3	0.83	0.09	10.7
Ctalamochita	1.00	0.23	4.3	0.80	0.04	25.6
Xanaes	1.00	0.05	18.3	0.58	0.48	2.1
Anisacate	1.00	0.19	5.3	0.69	0.23	16
Suquía	0.94	0.05	18.3	0.61	0.15	6.7
Dulce	0.78	0.05	21.3	0.56	0.12	8.5
Juramento	1.00	0.20	5.1	0.93	0.03	32
Bermejo	0.99	0.04	25.6	0.31	0.20	5.1
Pilcomayo	0.31	0.19	5.33	0.29	0.45	2.21
Paraná	0.83	0.12	8.5	0.41	0.03	32
Salado	0.93	0.22	4.6	0.69	0.44	2.3

In Figures 6, 11, 12 and 15, the first dominant frequency of the spectrum is marked with a rectangle. These frequencies (greater than the length of the series) were not taken into account because they are the product of trends in the series, or components of the low frequency of the series. This was demonstrated by analyzing synthetic series.

It can be observed in Table 3 that the two dominant periods occurred in the following ranges:

< 3.7 years 2 cases;
3.7 - 6.7 years 9 cases
8.5 - 10.7 years 4 cases
10.7 – 18.3 years 2 cases
18.3 – 32 years 11 cases

Table 3. Dominant frequencies of some of the basins studied.

Basin	Fourier		Wavelet	
	Period (years)	Period (years)	Period (years)	Period (years)
Atuel	4.7	10.7	4.1	23.4
Ctalamochita	4.3	25.6	4.1	23.4
Anisacate	5.3	16	5.8	16.5
Suquía	18.3	6.7	16.5	4.1
Dulce	21.3	8.5	8.3	23.4
Paraná	8.5	32	8.3	33.1

It is observed that most of the basins (except Colorado, Paraná and Dulce) show fluctuations with dominant periods between 3 and 7 years. Mean flow series of the Colorado, Paraná, Atuel and Dulce rivers have dominant periods between 7 and 11 years. Dominant periods between 13 and 35 years are observed in all river basins (except Atuel, Salado and Pilcomayo basins). Similar results were observed by other authors. For example, Vargas, Minetti and Poblete (2002) observed quasi-periodic low frequency fluctuations (22 to 26 years) in the mean annual flow series of Paraná River. Compagnucci, Berman, Velasco-Herrera and Silvestri (2014)observed periodicities of 3.5 in the mean annual flow series of Paraná River corresponding to 9 and 30 years, and for Atuel River periodicities of 4-5 years, corresponding to 7, 11 and 22 years.

In the case of San Juan River, five frequency bands with significant amplitudes were observed, corresponding to periods of approximately 12.3, 7.4, 5.7 and 3.8 years (Correa & Guevara, 1992).

Wavelet coherence analysis

A wavelet coherence analysis was performed for the mean annual flow series, in order to validate the results obtained with the Fourier spectral analysis. In the case of signals that present multiple scales of temporal and spatial variability and frequency, a localized analysis of transformations with wavelet curves can be useful to identify the dominant geometries of the variables analyzed. With regard to dominant frequencies, similar results were obtained with spectral analysis methodologies based on the Fourier transform and wavelet curves. This shows that the signals analyzed do not have a high degree of variability in dominant frequencies, and therefore, satisfactory results would be achieved with the application of the Fourier-based spectral analysis.

The analysis was performed using Morlet wavelet function (*ko* = 6).

Analysis of the contribution of different processes to the fluctuations observed in the flow series

The analysis of dominant frequencies for mean annual flow series enabled observing the predominant frequency ranges. Then, the variance was calculated (Figure 16). The variance is computed by integrating the energy spectrum in the frequency range analyzed. It allows evaluating the contribution of the fluctuation variances of each frequency range, which is a characteristic of the different processes. Band-pass filters were applied to the energy spectrum between the following frequency ranges:

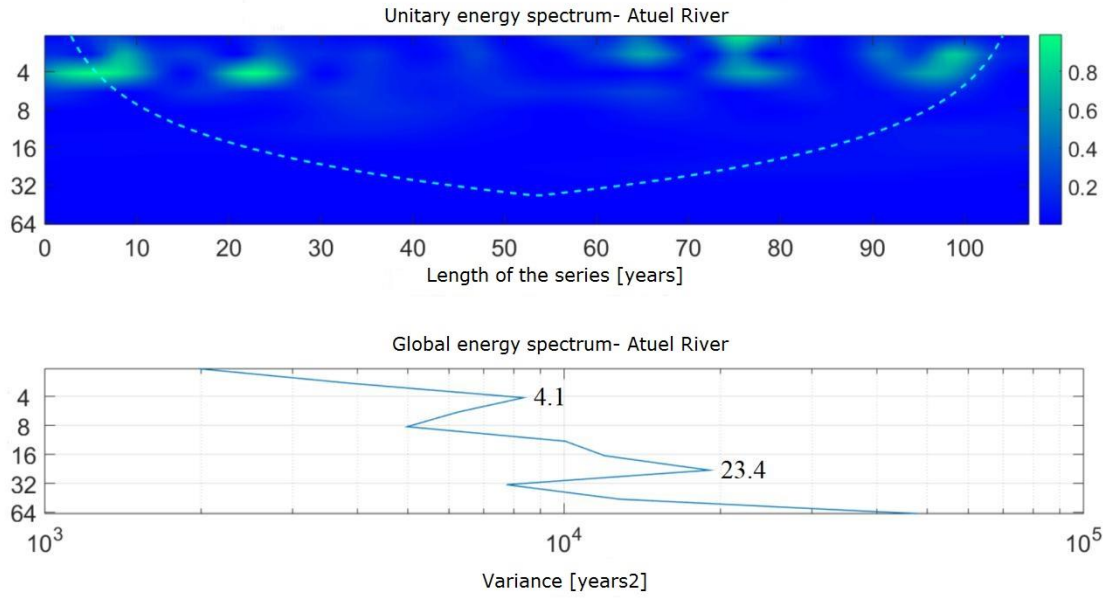

Figure 16. Spectrum of unitary and global energy of mean annual flow series of Atuel River.

N_a: periods of fluctuations less than 2.2 years and represents random variability.

N_2: periods of fluctuations between 2.2 and 3 years

N_5: periods of fluctuations between 2.2 and 3 years

N_{11}: periods of fluctuations between 3-7 years

N_{bd}: periods of fluctuations between 7-13 years

N_v: periods of fluctuations greater than 35 years

The band-pass filter used in this paper consisted of a Fourier filter. First, the tool was verified with the analysis of a synthetic series (fluctuations of known periods), making the energy of the fluctuations equal to zero for the frequency ranges not included in the band of the band-pass filter used. Table 4 summarizes the results, indicating the contribution to the total variance of the fluctuations of each frequency range.

Table 4. Contribution to the total variance of mean annual flow fluctuations, in each bandwidth.

Basin	Total variance of the fluctuations of the mean annual flow series in each bandwidth						
	N_a	N_2	N_5	N_{11}	N_{bd}	N_{vc}	Sum

San Juan	45%	3%	27%	5%	4%	7%	87
Mendoza	40%	0%	9%	3%	20%	3%	75
Atuel	36%	2%	23%	9%	15%	11%	96
Colorado	50%	8%	12%	11%	10%	1%	92
Ctalamochita	50%	0%	19%	8%	19%	0%	96
Xanaes	43%	0%	9%	8%	15%	9%	84
Anisacate	19%	2%	38%	12%	5%	0%	76
Suquía	38%	0%	14%	8%	15%	15%	90
Dulce	28%	6%	4%	16%	25%	16%	95
Juramento	49%	12%	22%	1%	12%	0%	96
Bermejo	27%	4%	19%	3%	23%	20%	96
Pilcomayo	33%	6%	9%	4%	26%	0%	78
Paraná	31%	3%	16%	21%	9%	16%	96
Salado	30%	5%	36%	2%	2%	2%	77

The sum is different than 100% because of the correlation between the components.

In N_a, processes less than 2.2 years and the random part of all frequencies are considered. Correa and Guevara (1992) proposed that residual variance not explained by significant periodicities should be attributed to the stochastic component. This random variance in 86% of the study cases represents between 30% and 50% of the variance of the fluctuations. Thus, the series has a high random component. The rest can be explained by different processes, with characteristic frequencies between 2 and 3 years, 3 and 7 years, 7 and 13 years, 13 and 35 years, and greater than 35 years.

Table 4 shows 9 basins (of 14 studied) where the low frequency processes N_{bd} dominated (without considering the Na processes), followed in importance by N_5. For two basins, the N_v process was notable, and the N_{11} process was notable for only one (Paraná). This result shows fluctuations of high, low and medium frequency in the mean annual flow series analyzed, which contribute, with different significance, to the temporal variability of drained flows. This result allows to advance in the study of processes that should be considered in the explanation of hydrological phenomena such as droughts and water excesses, taking into account that the process involves phenomena that have a temporal evolution that includes small, medium and large scales, and random or stochastic processes.

Relation between temporal evolution of hydrological droughts and macro-climatic indices

In this section, macro-climatic and astronomical indices are analyzed using the same spectral analysis of time series, to determine whether there is a relationship between its temporal evolution with the hydrological droughts in the different time scales.

Table 5i describes the macro-climatic indices analyzed.

Table 5. Summary of analyzed macro-climatic indices.

Index	Description	Period
TNA	Tropical North Atlantic Index	1948-2013
TSA	Tropical South Atlantic Index	1948-2013
AMO	Atlantic Multidecadal Oscillation	1861-2008
AMM	Southern Meridional Mode	1948-2001
SOI	South Oscillation Index	1951-2013
PDO	Decadal Oscillation of the Pacific	1948-2013
MS	Sunspots	1700-2013
ONI	Oceanic Niño Index	1950-2012
Niño 3.4	Mean sea surface temperature in Niño 3 and Niño 4 regions	1950-2013
Niño 1+2	Mean sea surface temperature in Niño 2+1 regions	1950-2013

The selected indices are: ONI, AMM, TSA, AMO, SOI, PDO, Niño 1+2; Niño 3.4 and TNA (see Table 5). Table 5 and Table 6 show the observed dominant periods of the fluctuations and the contributions to the variance (in percentage) of the fluctuations, with the different bandwidths analyzed previously.

Table 6. Dominant periods in each series of indices analyzed.

Index		MS	AMO	AMM	ONI	PDO	SOI	NIÑO 3.4	NIÑO 1+2	TSA	TNA
Period	1st maximum selected value [years]	10.9	64.0	9.1	4.9	21.0	12.8	4.9	4.9	11.6	8.5
	2nd maximum selected value	10.0	32.0	2.9	3.6	5.6	4.9	3.5	3.5	21.3	21.5

	[years]										

Time series of AMO, AMM, ONI, PDO, SOI, Niño 3.4, Niño 1 + 2, TSA and TNA indices were obtained from the NOAA website NOAA (2016), and sunspot time series were obtained from SILSO SILSO (2016).

In the PDO, TNA, AMM indices, a dominant frequency of 64 years^{-1} was observed, and 128 years^{-1} for the TSA index. However, they were discarded because of great uncertainty, since the series have a length less than 100 years. This analysis shows a dominant frequency on the order of 4 to 5 years for Niño 1+2, Niño 3.4 and ONI indices. The Sunspots, AMM, SOI, TSA and TNA index have dominant frequencies between 8.5 and 13 years. While the PDO and AMO indices have a dominant multidecadal frequency.

Table 7 shows that the n_{11} processes contribute 66% to the variance of the energy spectrum, while process n_5 has an important contribution in the ONI, Niño 3.4 and Niño 1+2 indices.

Table 7. Contribution of the variance, in percentage, to the different bandwidths analyzed.

	MS	AMO	AMM	ONI	PDO	SOI	NIÑO 3.4	NIÑO 1+2	TSA	TNA
N_a	2%	1%	56%	52%	21%	44%	49%	64%	43 %	52%
N_5	4%	0%	0%	40%	19%	25%	38%	34%	5%	0%
N_{11}	66%	1%	18%	6%	14%	18%	6%	0%	12 %	14%
N_{bd}	5%	10%	1%	0%	9%	2%	0%	0%	7%	5%
N_v	20%	86%	3%	0%	29%	0%	0%	0%	25 %	21%

Analysis of correlation between fluctuations of mean annual flow series and macro-climatic indices

Knowing the macro-climatic indices, whose fluctuations can be linked to droughts on different time scales, helps the prediction of these phenomena. In this section, the correlation between fluctuations of mean annual flow series and macro-climatic indices (for different bandwidths) is analyzed. The basins selected for this analysis are Suquía, Dulce, Paraná, San Juan and Atuel rivers, because they are

the most extensive and representative time series of each study region. The Fourier band-pass filters used in this analysis are N_{bd} (between 13 and 35 years), N_{11} (between 7 and 13 years) and N_5 (between 3 and 7 years). In this analysis, the correlation coefficient between the flow filtered time series of each basin (N_{bd}, N_{11}, N_5) and the macro-climatic indices filtered series was calculated with the same bandwidth. Then, the series with the best correlation coefficients were graphed. Below are the results for the basins analyzed.

Dulce River

Table 8 shows the correlation coefficient between the series of flows of the Dulce River and the series of the different indicators.

Table 8. Correlation coefficient between Dulce River mean flow series and different indices series.

n_{bd}									
TNA	MS	AMO	ONI	PDO	SOI	AMM	NIÑO 3.4	NIÑO 1+2	TSA
0.46	0.59	0.63	0.23	0.71	-0.32	0.82	0.16	0.73	-0.51
n_{11}									
TNA	MS	AMO	ONI	PDO	SOI	AMM	NIÑO 3.4	NIÑO 1+2	TSA
-0.40	-0.08	0.28	-0.44	-0.36	0.19	-0.21	-0.42	0.42	-0.03
n_5									
TNA	MS	AMO	ONI	PDO	SOI	AMM	NIÑO 3.4	NIÑO 1+2	TSA
0.54	0.20	-0.33	0.37	0.46	-0.29	0.39	0.38	0.19	0.25

The temporal evolution of the mean annual flow series and the macro-climatic indices are shown in the following figures. In order to plot the mean flow series, these series were normalized by subtracting the mean value and dividing by the deviation of each series.

Figure 17a shows that the negative phase of the AMM index coincides with severe droughts in the basin in the 40's, 60's, late 80's and the drought in the years 2011 and 2013. The high correlation observed between the mean flow series and the MS, AMO, PDO, Niño 1+2 and TSA indices for the bandwidth of 13-35 years is notable. Figure 17b

shows that Niño 1+2 index in its negative phase is succeeded after two years by periods of droughts in the basin. This behavior is observed in drought events in the 50's and 60's (severe droughts due to their permanence over time), and during 1988-1989, 1993-1995, 2002-2004 and 2011-2013. Figure 17e shows a correspondence between valleys and peaks for most of the observed cycles, except for the period 1994-2004. Figure 18 shows that the positive phases of the TSA index coincide with drought events occurring in 1962-1971, and precede the 1988-1990 and 2005-2010 droughts. It is noted that since 1950, these droughts were the longest identified to date.

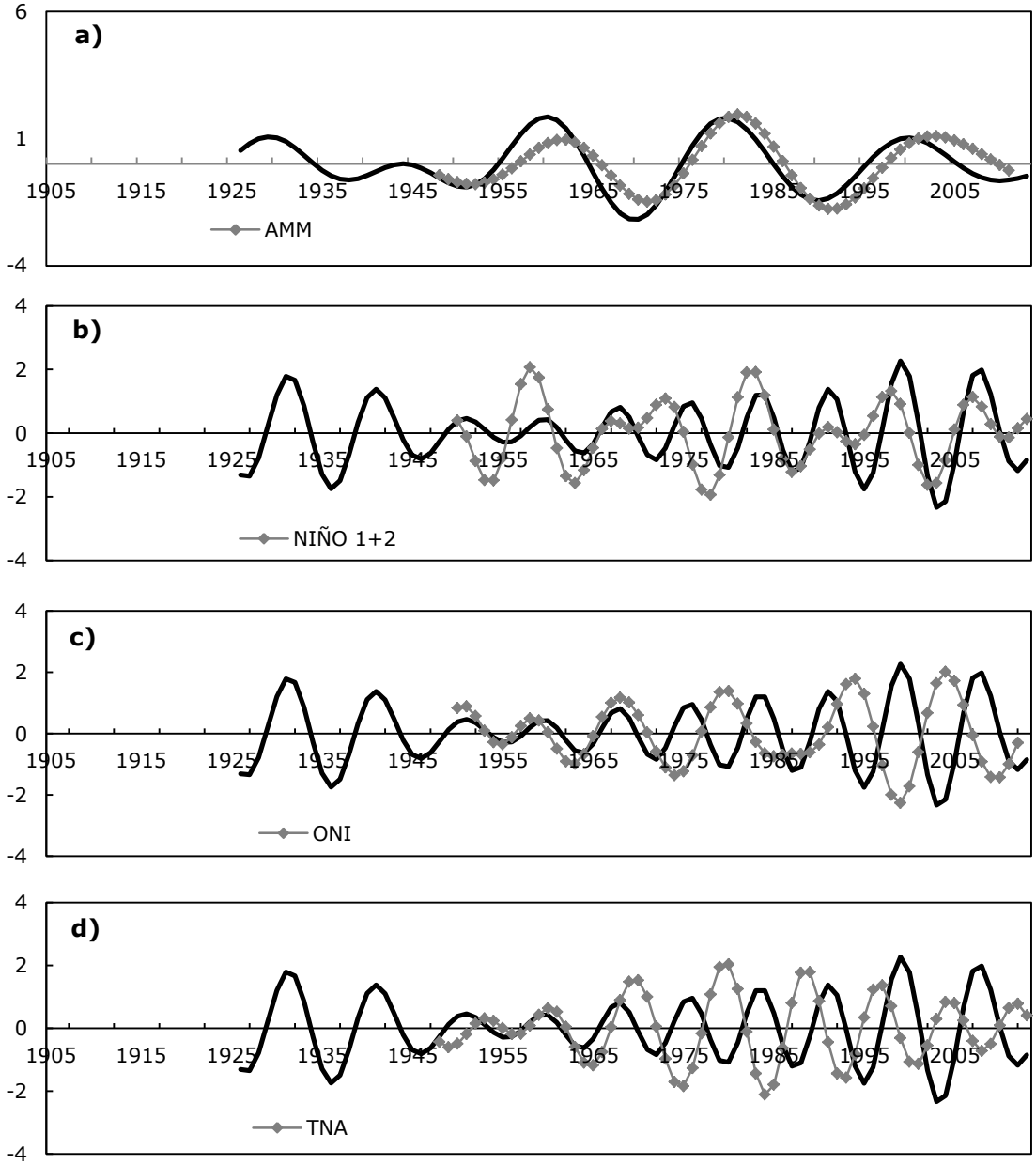

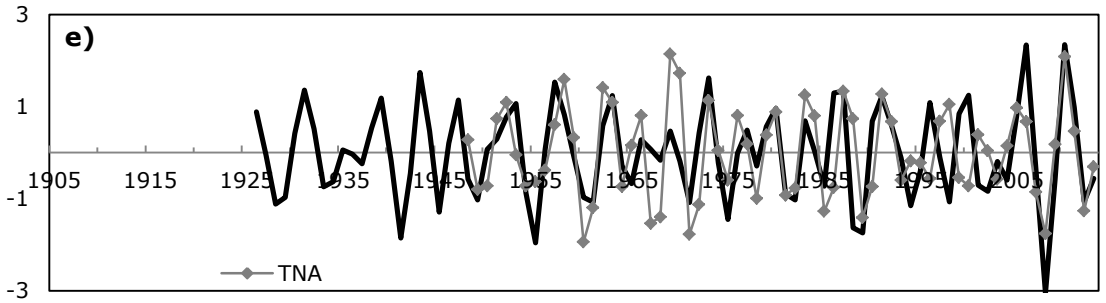

Figure 17. a) Dulce River mean annual flow series and AMM index, both filtered using a band-pass filter between 13-35 years. Normalized flow of Dulce River with band-pass filter between 7-13 years and Niño 1+2 index b) ONI index c) and d) TNA index e) Dulce River mean annual flow and TNA index, both filtered with a band-pass filter between 3-7 years.

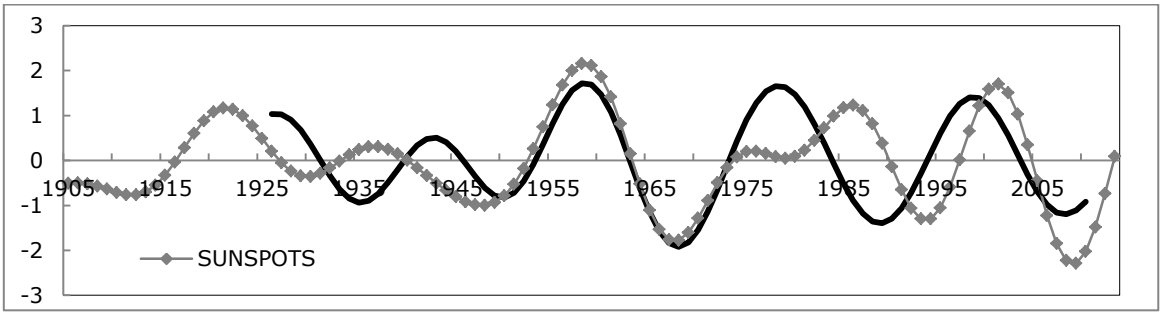

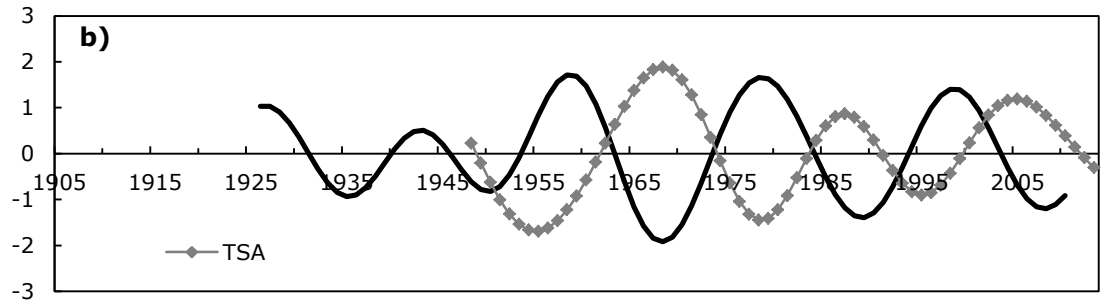

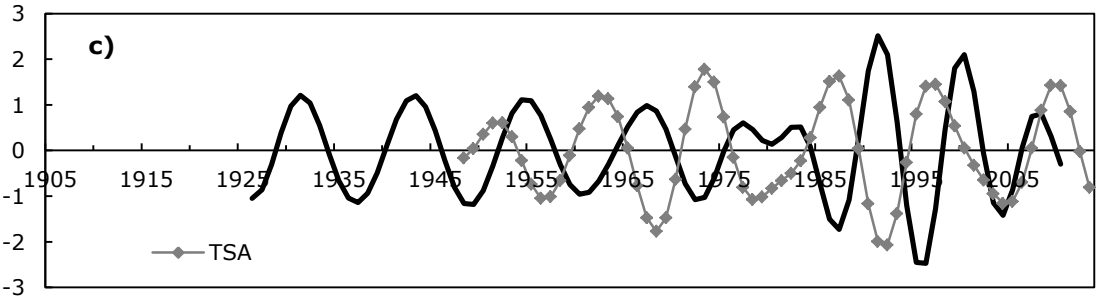

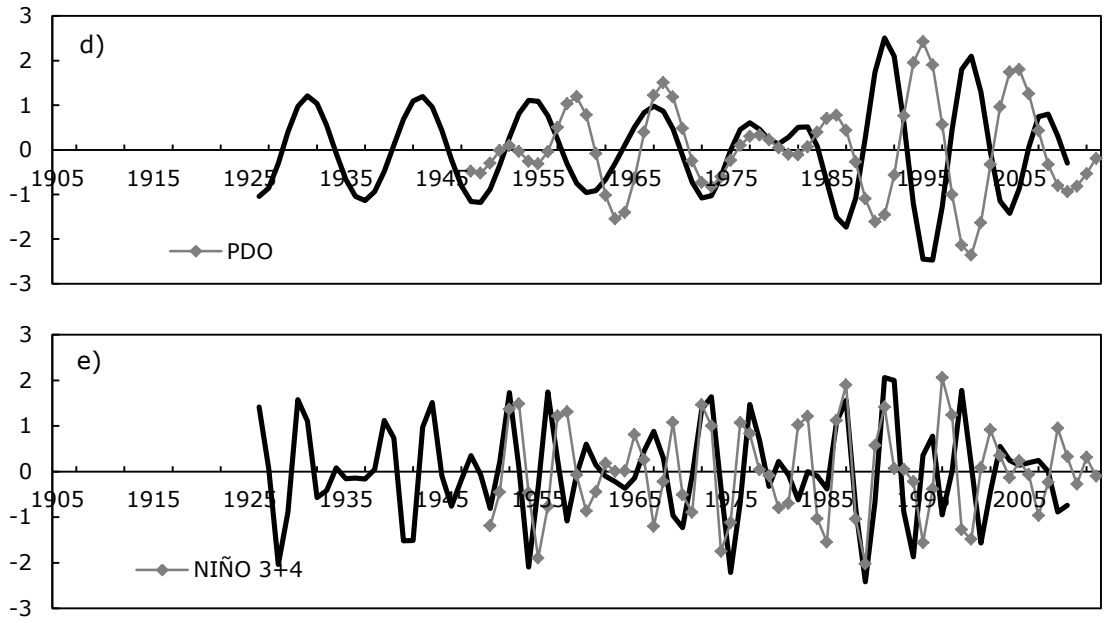

Figure 18. Suquia river mean flow series and Sunspots index a) and TSA index b) all filtered using band-pass filter between 13-35 years. Suquía River mean flow series and TSA index c) PDO index d) all filtered using band-pass filter between 7-13 years; e) Suquía River mean flow series and Niño 3.4 index, both filtered using a band-pass filter between 3-7 years.

Figure 19a shows that the positive phase of the TSA index coincides with water deficits (1966-1972 drought) and periods of low mean flows (not identified as hydrological droughts) during the years 1985-1988 and 1999-2008. Figure 19c shows that the negative phases of Niño 1+2 index coincide with droughts during 1947-55 (in the final stage), 1961-63, 1977, 1995 and 2001-05, and with the stage of low flows in 1986-1988 (not identified as hydrological droughts). Figure 20a shows that the negative phases of the AMM index coincide with periods of water deficits in the basin corresponding to the droughts identified in 1945-1952, 1966-1971, 1988-1996 and 2009-2013. The negative phases of the Niño 3.4 index coincide with drought events in the basin during the years 1950-1951, 1960, 1962-1965, 1975, and low flow in 1985, 1988-1989, 1995-1996, 1999, 2004 and 2007 (see Figure 20c). Figure 21a shows that the negative phases of the AMM index coincide with the bi-decadal cycles of low flow observed in the San Juan River basin. During these negative phases, droughts were identified in 1945-53, 1966-75, 1988-96 and 2010-13. Figure 21d shows that the negative phases of the Niño 3.4 index coincide with most of the drought events identified. These events are: 1954-57, 1960-62, 1964, 1974-75, 1979-81, 1985, 1988-89, 1993-96, 1999 and 2007-08.

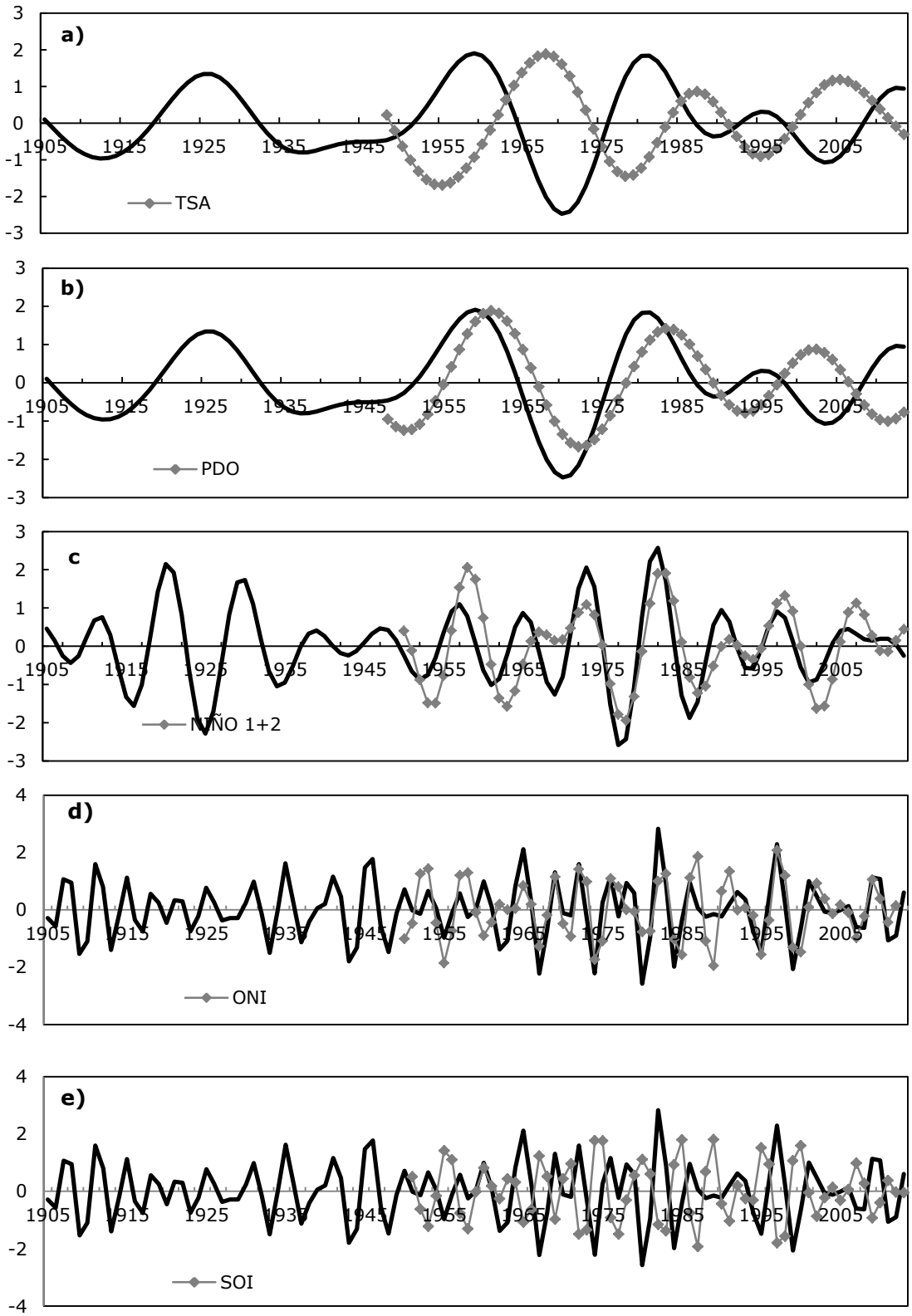

Figure 19. Paraná River mean flow series and TSA index a) and PDO index b) all filtered using band-pass filter between 13-35 years; c) Paraná River mean flow series and Niño 1+2 index, filtered using band-pass filter between 7-13 years;

Paraná River mean flow series and ONI index d) and SOI index e); all filtered using band-pass filter between 3-7 years.

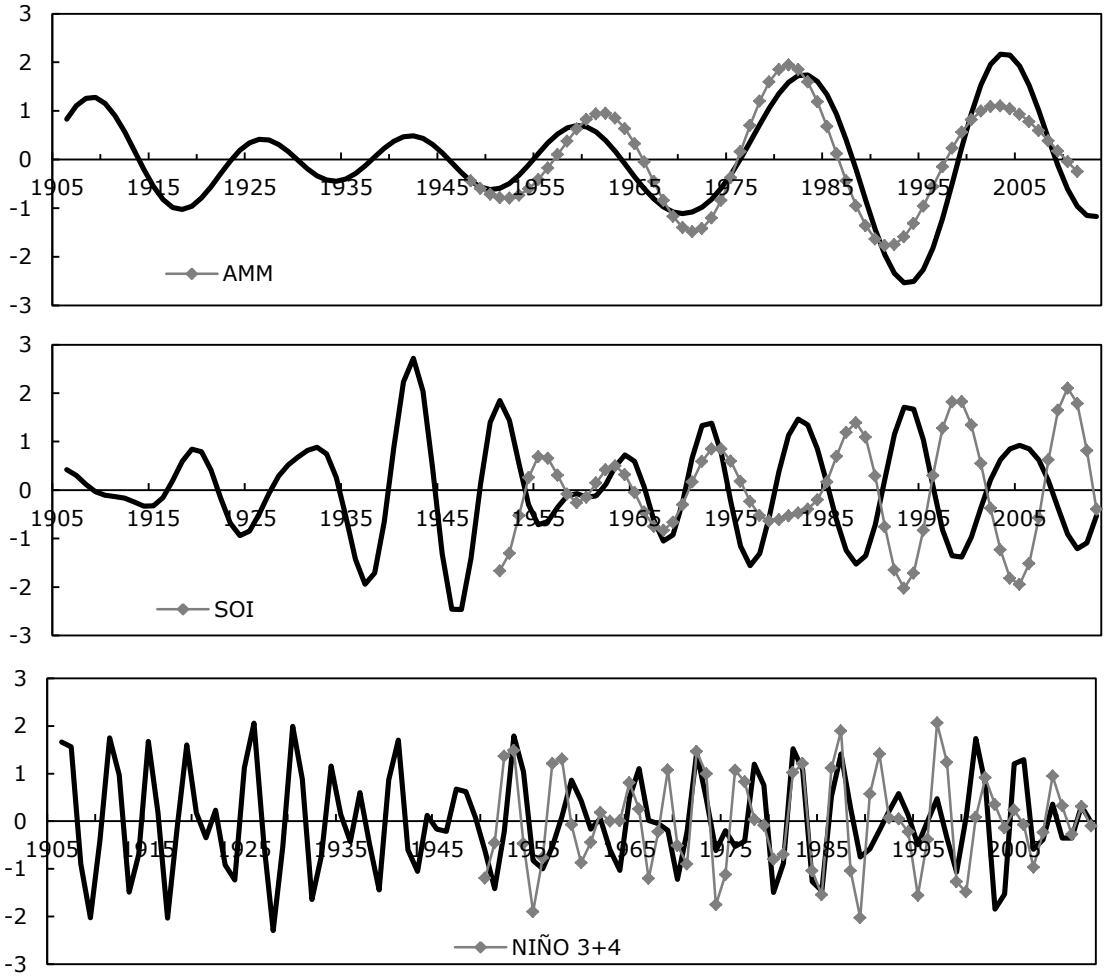

Figure 20. a) Atuel River mean flow series and AMM index. Both filtered using band-pass filter between 13-35 years; b) Atuel River mean flow series and SOI index, both filtered using band-pass filter between 7-13 years; c) Atuel River mean flow series and Niño 3.4 index, both filtered using band-pass filter between 3-7 years.

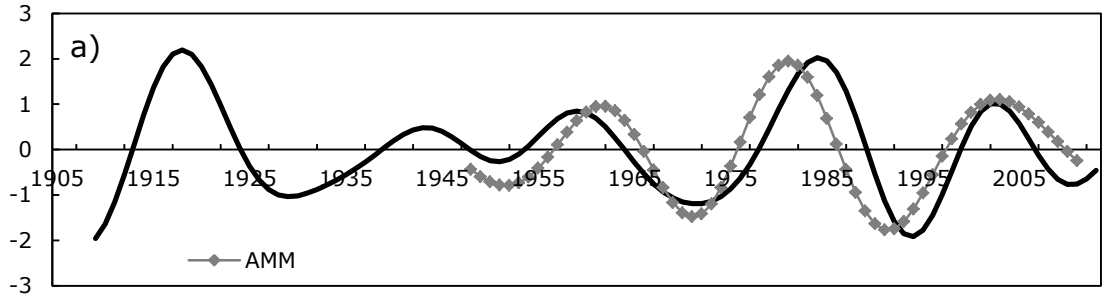

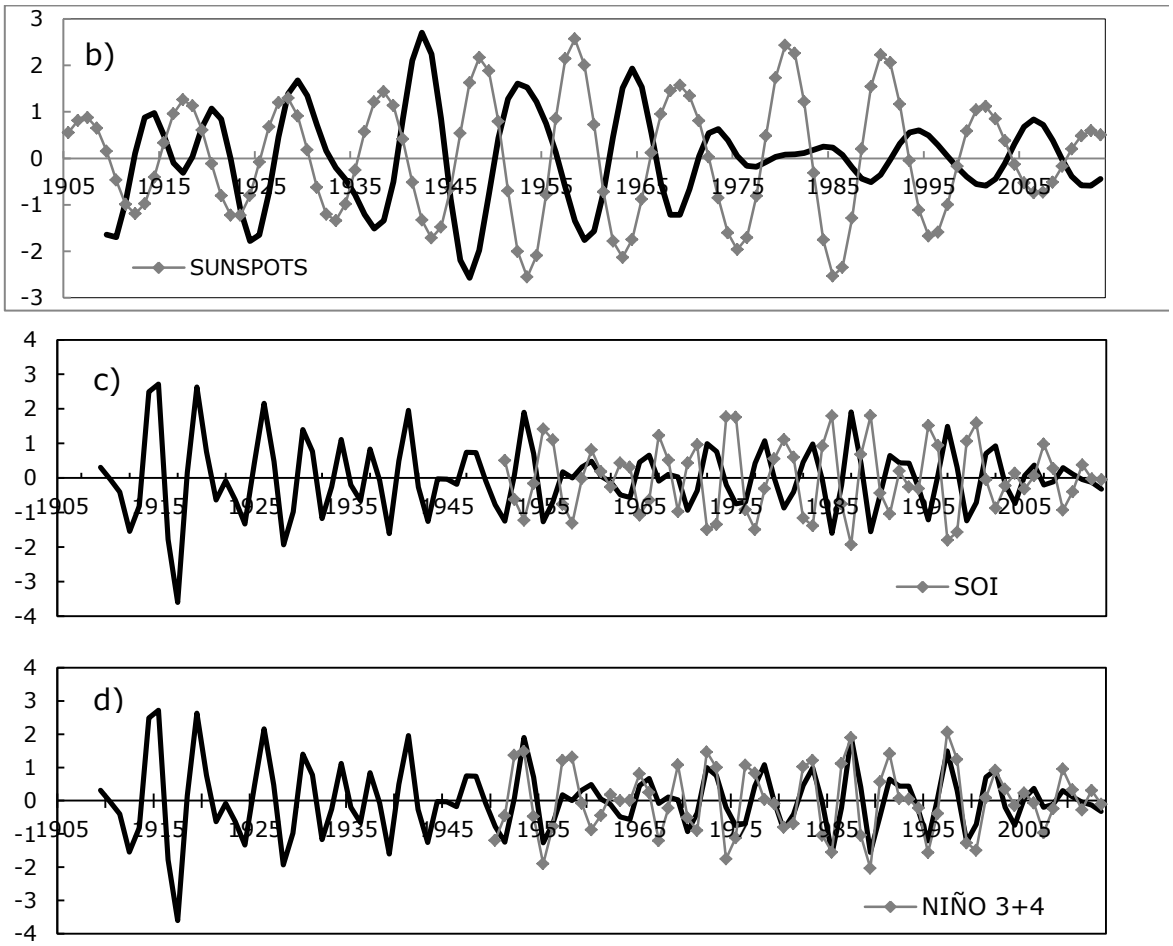

Figure 21. a) San Juan River mean flow series and AMM index both filtered using band-pass filter between 13-35 years; b) San Juan River mean flow series and sun spot series, both filtered using band-pass filter between 7-13 years; c) San Juan River mean flow series and SOI index, both filtered using band-pass filter between 3-7 years; d) San Juan River mean flow series and Niño 3.4 index, both filtered using band-pass filter between 3-7 years.

Suquía River

Table 9 shows correlation coefficient between Suquía River mean flow series and different index series.

Table 9. Correlation coefficient between Suquía River mean flow series and different index series.

Nbd									
TNA	MS	AMO	ONI	PDO	SOI	AMM	NIÑO 3.4	NIÑO 1+2	TSA
0.09	0.59	0.25	-0.01	0.39	-0.15	0.51	-0.16	0.58	-0.74

n11									
TNA	MS	AMO	ONI	PDO	SOI	AMM	NIÑO 3.4	NIÑO 1+2	TSA
-0.21	0.11	0.28	-0.15	-0.51	0.00	0.01	-0.13	0.01	-0.53
n5									
TNA	MS	AMO	ONI	PDO	SOI	AMM	NIÑO 3.4	NIÑO 1+2	TSA
0.03	-0.09	-0.04	0.20	0.05	-0.15	-0.08	0.22	0.12	0.19

Paraná River

Table 10 shows correlation coefficient between Paraná River mean annual flow series and different index series.

Table 10. Correlation coefficient between Paraná River mean annual flow series and different index series.

n_{bd}									
TNA	MS	AMO	ONI	PDO	SOI	AMM	NIÑO 3.4	NIÑO 1+2	TSA
0.36	0.45	0.39	0.36	0.54	-0.53	0.53	0.13	0.27	-0.69
n_{11}									
TNA	MS	AMO	ONI	PDO	SOI	AMM	NIÑO 3.4	NIÑO 1+2	TSA
-0.06	0.17	0.11	-0.13	-0.19	0.13	-0.09	-0.06	0.68	0.07
n_5									
TNA	MS	AMO	ONI	PDO	SOI	AMM	NIÑO 3.4	NIÑO 1+2	TSA
0.07	-0.28	-0.03	0.60	0.34	-0.59	-0.07	0.58	0.57	-0.34

In the following figures, the most significant ones are presented.

Atuel River

Table 11 shows correlation coefficient between Atuel river mean flow series and different index series.

Table 11. Correlation coefficient between Atuel river mean flow series and different index series.

n_{bd}									
TNA	SOL	AMO	ONI	PDO	SOI	AMM	NIÑO 3.4	NIÑO 1+2	TSA
0.62	0.37	0.64	0.02	0.65	-0.02	0.87	0.08	0.42	0.06
n_{11}									
TNA	SOL	AMO	ONI	PDO	SOI	AMM	NIÑO 3.4	NIÑO 1+2	TSA
-0.34	-0.27	0.24	0.43	0.22	-0.62	-0.41	0.41	0.22	0.00
n_5									
TNA	SOL	AMO	ONI	PDO	SOI	AMM	NIÑO 3.4	NIÑO 1+2	TSA
0.05	-0.11	0.11	0.45	0.26	-0.50	-0.14	0.46	0.38	-0.14

The following figures present the most significant results.

San Juan River

Table 12 shoes correlation coefficient between San Juan River mean flow series and different index series.

Table 12. Correlation coefficient between San Juan River mean flow series and different index series.

n_{bd}									
TNA	MS	AMO	ONI	PDO	SOI	AMM	NIÑO 3+4	NIÑO 1+2	TSA
0.39	0.49	0.30	0.19	0.63	-0.29	0.81	0.14	0.42	-0.15
n_{11}									
TNA	MS	AMO	ONI	PDO	SOI	AMM	NIÑO 3+4	NIÑO 1+2	TSA
-0.27	-0.46	0.36	0.04	-0.07	-0.22	-0.32	-0.05	-0.30	0.20
n_5									
TNA	MS	AMO	ONI	PDO	SOI	AMM	NIÑO 3+4	NIÑO 1+2	TSA
0.23	-0.23	0.07	0.69	0.60	-0.72	-0.16	0.70	0.62	0.05

Conclusion

This paper identifies multiannual periodicities observed in mean annual flow series corresponding to different fluvial systems in Argentina. The spectral analysis demonstrates that for 86% of the mean flow series, a random component (high frequency) explains around a 30% and 50% of the flow signals. In addition, variability in high, low and medium frequency series is observed, which contributes to flow fluctuations in different percentages. After the random component, predominant processes are those with dominant periods between 3 and 7 years (for example ENSO) and between 13 and 35 years (bidecadale oscillations). The results obtained in this work allow to advance in the study of the processes that should be considered in the explanation of hydrological phenomena such as droughts and excesses.

The Atlantic Ocean was found to have a large influence on bidecadal oscillations of mean flow series. In five of the basins analyzed, a high correlation between bidecadadal scales and AMM index was observed in the Dulce River (0.82), Paraná River (0.53), Atuel River (0.87), San Juan River (0.81) and Suquía River (0.51). The Paraná and Suquía rivers' mean flow series have a high negative correlation with the TSA index (Parana River -0.69; Suquía River -0.74).

On the decadal scale, significant correlations were observed (greater than 0.5) for Paraná River with Niño 1+2 index (0.68), Atuel River with SOI index (-0.62) and Suquía River with TSA index (-0.53).

On a multi-year scale, negative correlations were observed with SOI index for Paraná River (-0.59), Atuel River (-0.50) and San Juan River (-0.72), and strong positive correlations were found with the ONI index for Paraná River (0.60), with Niño 3.4 index for San Juan River and Atuel River (0.70, 0.46 respectively), and with the TNA index for Dulce River (0.54).

This confirms the results of previous works (Compagnucci *et al*., 2014; Mauas, Buccino y Flamenco, 2011; Dölling, 2014; Vargas *et al*., 2002) and provides new information about the links with Atlantic Ocean index for the different basins. These results are important for the understanding of macro-climatic dynamics in Argentina and its forecast in space and time.

Acknowledgment

Thank you to the National Council of Scientific and Technical Investigations of Argentina (CONICET) for the scholarship awarded to develop this work.